Structure and Morphology of Poly(diethyl trimethylene-1,1-dicarboxylate) Crystals

Pawel Sikorski,[†] Edward D. T. Atkins,*[,†] Lawino C. Kagumba,[‡] and Jacques Penelle[‡]

H. H. Wills Physics Laboratory, University of Bristol, Tyndall Avenue, Bristol BS8 1TL, U.K., and Department of Polymer Science and Engineering, University of Massachusetts, Amherst, Massachusetts 01003-4530

Received March 27, 2002; Revised Manuscript Received June 3, 2002

ABSTRACT: Poly(diethyl trimethylene-1,1-dicarboxylate) oligomers with an average degree of polymerization (DP) of 20 and a polydispersity of 1.13 have been isothermally crystallized at 30 °C from benzene and also crystallized from the melt (T_m = 176 °C). The crystals were investigated using electron microscopy (imaging and diffraction), X-ray diffraction, and computational modeling. The diffraction signals index on an orthorhombic unit cell with parameters $a = 1.554 \pm 0.002$ nm, $b = 1.136 \pm 0.002$ nm, and c (chain axis) $= 0.585 \pm 0.002$ nm. A space group of $P2_12_12_1$ is assigned on the basis of systematic absences of $h00$, $0k0$, and $00l$ for odd h, k, and l respectively; thus, two antiparallel chain segments pass through the basal ab plane of the unit cell. The calculated density of 1.20 g·cm^{-3} is commensurate with the measured value of 1.17 ± 0.03 g·cm^{-3}. The repetitive $-CH_2-CH_2-CX_2-$ backbone conformation, where the side groups X are ethyl esters ($-COOC_2H_5$), has the torsional angle sequence $GT\bar{G}G\bar{T}\bar{G}$ with the trans bonds at the dimethylene $C-CH_2-CH_2-C$ sites. This conformation generates a 2-fold helix with a pitch that matches the measured crystallographic c-value of 0.585 nm. Ellipsoidal-shaped, lamellar-like crystals, with lateral dimensions on the micron scale but only 7.23 nm thick, are obtained by isothermal crystallization from benzene at 30 °C. Electron and X-ray diffraction data show that the molecular axes are orthogonal to the lamellar surface and that the crystal thickness matches a DP of 20. Thus, a degree of selective crystallization of molecular length occurs in these solution-grown crystals at fixed temperature. Under appropriate conditions, the crystals also stack to generate a one-dimensional lattice. This feature does not occur in the melt-crystallized fibers; in this case, the lamellar-like character is suppressed as the polydisperse molecules interpenetrate to form a crystal with a greater coherence length in the c-direction but, of course, with chain-end defects.

Introduction

In 1942, Charles W. Bunn[1] described the various types of conformation for an alkane chain. He described some of the basic chain conformations generated using combinations of the three values 180°, +60°, and −60° for the backbone C−C bond torsion angles that correspond to localized potential energy minima. We now use the notation trans (T), gauche plus (G), and gauche minus ($\bar{G}$), respectively.[2] The most highly extended arrangement is, of course, the all-trans (TT) conformation, characteristic of crystalline polyethylene.[1] The introduction of gauche bonds into the backbone naturally reduces the axially projected advance (along the c-axis) per carbon atom. Each selected repetitive combination of trans and gauche bonds will generate a chain axis periodicity that will be a characteristic of that selection. In the polyethylene all-trans (TT) conformation, the stereochemical periodicity is 0.125 nm, and the conformation is a straightforward 2-fold helix, or all-trans conformation (planar zigzag), with a crystallographic c-axis repeat of 0.25 nm. The stereochemical periodicity will also, of course, be influenced by the frequency of side-group implantations. For example, in the case of isotactic polystyrene, the aromatic appendage on every second backbone carbon changes the backbone conformation to TG and generates a 3-fold helical conformation ($TGTGTG$)[3,4] and a c-axis repeat of 0.665 nm. Thus, the value of the c-repeat is a combination of side-group implantation frequency and the stereochemical nature of the side group.

In the case of poly(1,1-disubstituted trimethylene)s of general structure $[-CH_2-CH_2-CXY-]_n$, the side groups introduce a repetitive decoration pattern on every third backbone atom. For an all-trans ($TTTTTT$) polytrimethylene backbone conformation this would generate a 2-fold helical conformation with a c-repeat of 0.75 nm. Judging from NMR evidence, an all-trans structure has been proposed by Alder et al.[5] for oligo(fluoren-9,9-diyl-*alt*-ethane-1,2-diyl)s such as pentamer **1** (Scheme 1), where the substitution XY is a fused, essentially planar, aromatic entity arranged orthogonal to the c-axis. Alder et al.[6] have also discussed how the substituent side groups can possibly control local conformations on the polymeric backbone of systems similar to the one reported here.

In this contribution, we investigate poly(diethyl trimethylene-1,1-dicarboxylate), or PDTD, a polytrimethylene polymer for which the side substituents are ethyl ester ($X = Y = -COOC_2H_5$). Details of the synthesis and characterization of this and similarly substituted polymers have been recently reported.[7,8] The complete chemical structure of the PDTD molecules, including the terminal groups, is $Ph-S-[CH_2CH_2CX_2]_n-H$.

We find that the process of isothermal crystallization from solution selectively crystallizes molecules with a degree of polymerization (n) of 20 to form lamellar-like crystals with a thickness commensurate with the length

* Corresponding author. Fax: +44-117-925 5624. E-mail: e.atkins@bristol.ac.uk.
[†] University of Bristol.
[‡] University of Massachusetts-Amherst.

10.1021/ma020486z CCC: $22.00
Published on Web 07/27/2002

Scheme 1. Pentamer 1 from Alder et al.;[5,6] *c*-Axis Vertical

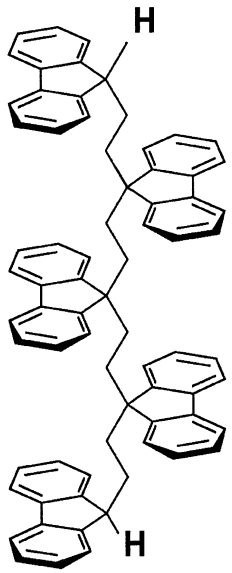

of the molecule. We are able to visualize the morphology of these crystals using transmission electron microscopy and undertake an analysis of the crystal structure using electron diffraction and X-ray diffraction data recorded from individual crystals and oriented crystal stacks, respectively.

Experimental Section

Materials. A PDTD sample [weight-average molecular weight ($\overline{M}_w$) = 3850, equivalent to a degree of polymerization (DP) of ≈20 and a polydispersity of 1.13] was synthesized via the anionic ring-opening polymerization of diethyl 1,1-cyclopropanedicarboxylate in the presence of sodium thiophenolate (PhSNa) initiator in DMSO at 130 °C.[7]

Preparation of Samples. *Isothermal Crystallization from Solution.* PDTD was dissolved in benzene (1% w/v) at 70 °C for 30 min. Crystals of the polymer were prepared by isothermal crystallization at 30 °C for 12 h before being cooled to room temperature. Oriented crystal mats suitable for X-ray diffraction were prepared by sucking the crystal suspension through a 0.2-μm Millipore filter using a water aspirator.

Crystallization from the Melt. Fibers suitable for X-ray diffraction were prepared by crystallization from the melt (T_m = 176 °C). Fibers were drawn from the melt and allowed to cool to room temperature. The density (ρ) was measured at 25 °C by flotation in a mixture of perfluorodecalin (ρ = 1.908 g·cm^{-3}) and pentane (ρ = 0.626 g·cm^{-3}). The density of crystalline PDTD was found to be 1.17 ± 0.03 g·cm^{-3}.

Transmission Electron Microscopy. Drops of the crystal suspension, diluted to a concentration of 0.01% w/v, were placed on carbon-coated transmission electron microscopy (TEM) grids and allowed to dry. Samples were shadowed with gold, and in some instances with Pt−Pd, to enhance the contrast of the TEM images. The diffraction ring from the gold coating was used to calibrate the electron diffraction patterns. TEM images and electron diffraction patterns were observed at room temperature using a JEOL 100 CX electron microscope operating at 100 kV.

X-ray Diffraction. Both wide- and low-angle X-ray diffraction patterns were obtained at room temperature using nickel-filtered Cu Kα radiation of wavelength 0.1542 nm from a Siemens sealed tube X-ray generator operating at 35 kV and 40 mA. The X-ray diffraction patterns were recorded using a point-collimated beam and a flat-plate image plate holder in evacuated cameras. Calcite (d_{111} = 0.3035 nm) was dusted onto selected samples for calibration purposes. X-ray diffraction patterns were obtained with the incident beam directed parallel and orthogonal to the mat surface for the solution-grown mats and also parallel and orthogonal to the film surface for the melt-cooled films.

Model Building and Analyses of Structure. *Torsional Angle Calculations.* The potential energy profiles for backbone torsional angles were calculated using the Insight II computer program and the CVFF force field. For each backbone bond, the torsion angles at the center of successive trimers of the PDTD molecule, translating one backbone carbon at a time, were examined. Scans were performed by setting the torsion angle under investigation at given values between 0° and 360° in 10° steps and minimizing the energy of the system.

Modeling. The software package Cerius2, version 3.8 (MSI), was used in the structural modeling and diffraction simulations. The basic strategy was to determine the molecular conformation of the PDTD molecule and the molecular packing arrangement within the experimental unit cell. After the initial model-building stage, a combination of energy minimization (EMin), using the CVFF force field, and simulation of diffraction patterns was used. It was ensured that the model was stereochemically sound and that the simulated diffraction patterns were in good agreement with the experimental data.

Diffraction Pattern Simulations. In the computer-simulated X-ray diffraction patterns, the temperature factor, degree of arcing, and relative intensity were chosen to match the experimental X-ray diffraction pattern(s). At each reciprocal lattice point, the calculated intensity was compared with the observed intensity to ensure that the final refined structure had no unacceptable discrepancies.[9]

Results

PDTD Lamellar Crystals. *Electron Microscopy.* Figure 1 shows PDTD lamellar-like crystals grown isothermally from a benzene solution. Figure 1a shows a common scene of gently overlaying lamellar-like crystals with no particular azimuthal interrelationship. In general, the crystals are crudely ellipsoidal in shape and a few microns in length. Figure 1b shows a higher-magnification image of two adjacent individual crystals for which the metal shadowing gives a value of 7−8 nm for the thickness. In some instances, PDTD crystals form a terraced stack in azimuthal register, as shown in Figure 1c (≈10 layers). It is probable that this type of architecture is a consequence of epitaxial crystallization. In some instances screw dislocations are a possibility, as illustrated in Figure 1d.

Electron Diffraction. The electron diffraction pattern taken with the beam normal to the lamellar crystal surface is shown in Figure 2a and c. X-ray diffraction results obtained from sedimented mats later indicated that this diffraction pattern is the weighted *hk*0 reciprocal lattice, i.e., the chains are normal to the lamellar surface. Upon calibration of the electron diffraction pattern, all of the electron diffraction spots can be indexed in terms of a rectangular real lattice with parameters a = 1.554 nm, b = 1.136 nm, and γ = 90°. The indexing, diffraction spacings, and estimated relative intensities are given in Table 1. The relative azimuthal orientation of the electron diffraction pattern to the crystals is shown by the inset in Figure 1b. There are systematic absences for *h*00 and 0*k*0 for odd *h* and *k*, respectively, a feature consistent with a *p*2*gg* two-dimensional space group. This, together with the strong intensities of the {110} diffraction signals, supports a model with molecules sited at the corners and center of the *ab* rectangular lattice.

X-ray Diffraction. The wide-angle pattern obtained from an oriented, sedimented mat of PDTD isothermally

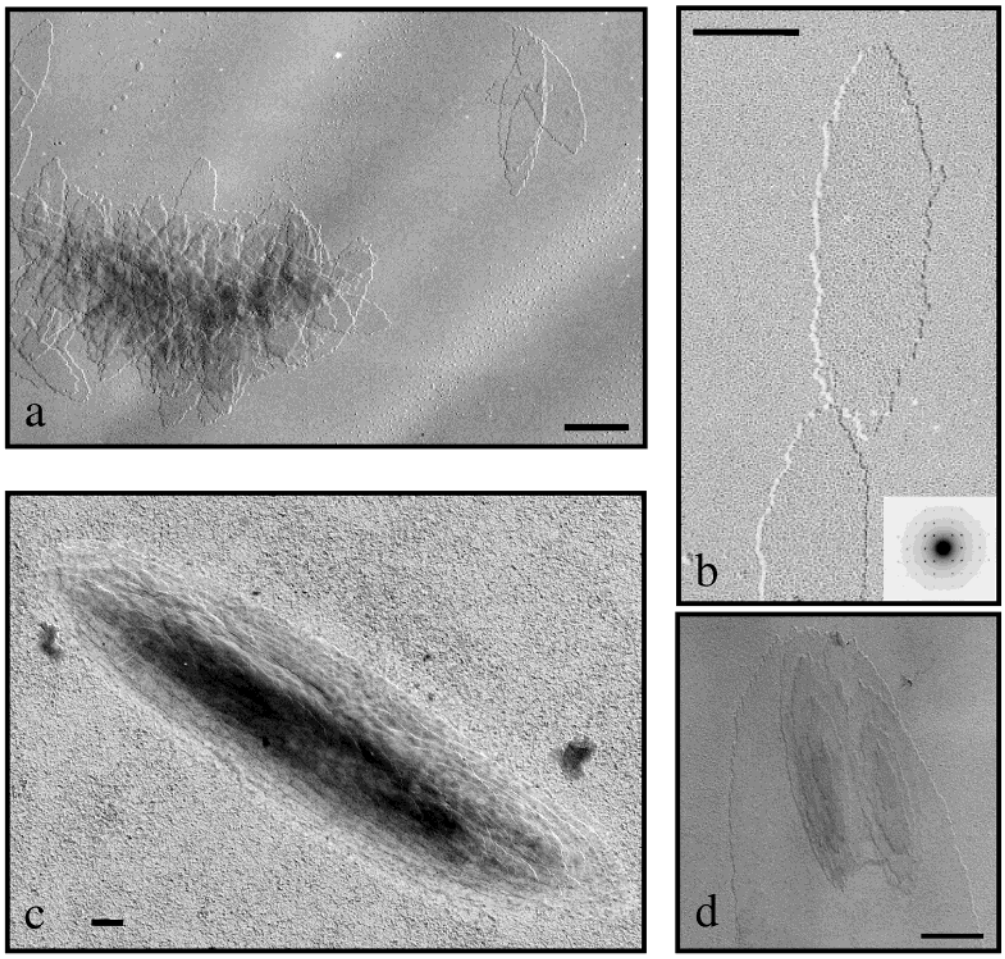

Figure 1. Transmission electron micrographs of the PDTD lamellar-like crystals isothermally crystallized from benzene; scale bars 1 μm. (a) Groups of the gently overlaid ellipsoidal crystals shadowed with gold to enhance contrast. (b) Pair of individual crystals at higher magnification, also shadowed with gold. Inset (lower right): Selected area (*hk*0) electron diffraction pattern taken with the electron beam normal to the lamellar surface to show the relative orientation with respect to the crystals. (c) Terraced stack (≈10 layers) of crystals in azimuthal register, shadowed with Pt−Pd. (d) Terracing with a suggestion of screw dislocations; gold shadowing.

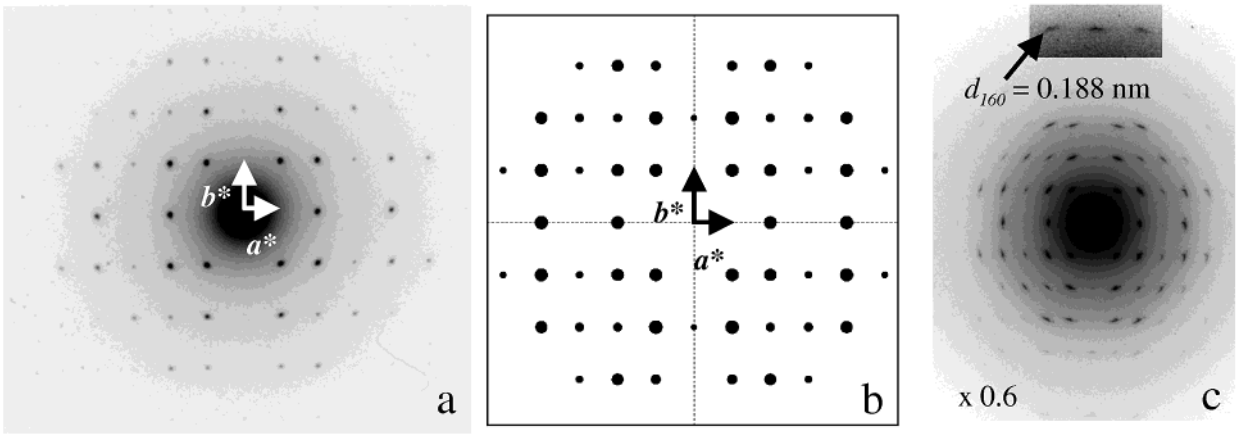

Figure 2. (a) Selected area *hk*0 electron diffraction pattern taken with the electron beam normal to the lamellar-like crystal surface (001). The diffraction signals index on a rectangular reciprocal lattice with $a^* = 0.644$ nm^{-1} and $b^* = 0.880$ nm^{-1} and the strong {110} family of diffraction signals suggest that the molecules are sited at the corner(s) and center of the *ab*-basal plane. The metal calibration ring is just visible on the periphery of the pattern. (b) Calculated weighted *hk*0 reciprocal net. The circular spot diameter is proportional to the relative intensity. (c) Reduced (60%) version of a; the signals reach a spacing of 0.188 nm as illustrated by the extra exposed region of the 160 signal (arrowed).

crystallized from benzene with the incident beam parallel to the mat surface (mat normal vertical) is shown in Figure 3a. There is cylindrical symmetry about the mat normal. Thus, although there is evidence of localized matching azimuthal orientation in limited stacks of lamellae (Figure 1c and d), in sedimented mats, there is no long-range azimuthal register between lamellae because mats are composed of either an individual

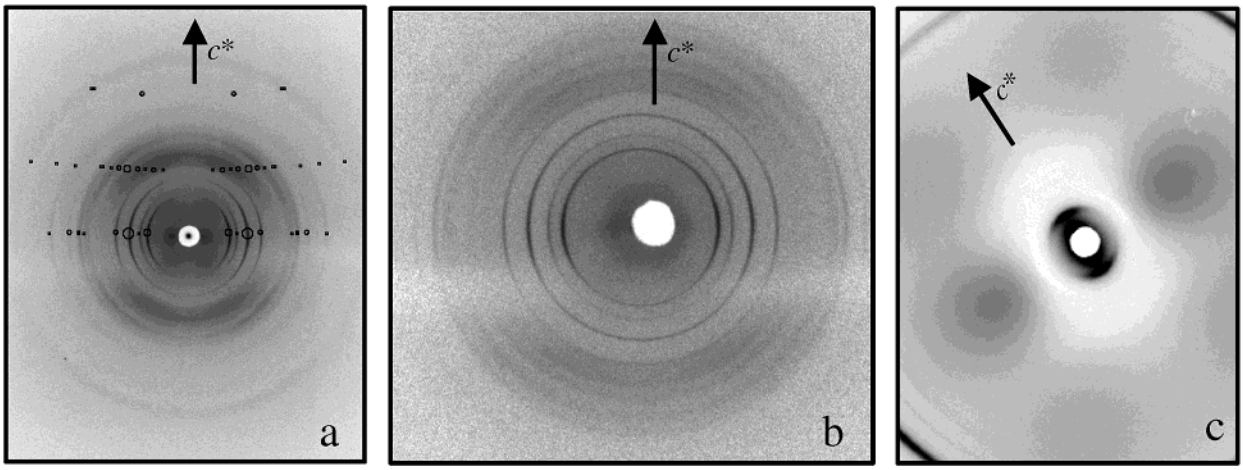

Figure 3. (a) Wide-angle X-ray diffraction pattern for PDTD isothermally crystallized from benzene and sedimented into oriented mats; the incident beam is directed parallel to the mat surface (mat normal vertical). The circles in the top half represent the calculated reciprocal lattice points; the diameters are proportional to the calculated relative intensities after appropriate Lorentz (incorporating Cox and Shaw factor) and polarization factors have been applied. (b) Wide-angle X-ray diffraction pattern from a melt-crystallized fiber of PDTD obtained with the incident beam directed orthogonal to the fiber axis (vertical). Note the increased sharpness of the first-layer-line diffraction signals. (c) Low-angle X-ray diffraction pattern showing a pair of diffraction arcs at a spacing of 7.26 ± 0.03 nm. The diffraction arcs near the periphery (top right-hand side and bottom left-hand side) are the wide-angle 110 diffraction signals, which provides a useful calibration.

Table 1. Electron Diffraction (*hk*0) Interplanar Spacings from Individual PDTD Lamellar Crystals

*hk*0[a]	d_{obs}[b]	d_{calc}	*hk*0[a]	d_{obs}[b]	d_{calc}
100	s	1.554	130/410	0.368	0.368
010	s	1.136	230	0.340	0.340
110	0.917	0.917	420	0.321	0.321
200	0.777	0.777	500	s	0.311
210	0.640	0.641	330	0.306	0.306
020	0.568	0.586	510	0.300	0.300
120	0.533	0.533	040	0.284	0.284
300	s	0.515	140	0.279	0.279
310	0.471	0.471	240	0.267	0.267
220	0.459	0.459	050	s	0.227
400	0.389	0.389	060	0.189	0.189
320	0.383	0.383	160	0.188	0.188
030	s	0.379			

[a] Indexed on a rectangular lattice with parameters $a = 1.554$ nm and $b = 1.136$ nm. [b] s = systematic absence.

Table 2. X-ray Diffraction Data from Oriented, Sedimented PDTD Lamellar-like Crystals

hkl[a]	d_{obs}[b]	d_{calc}	I_{obs}[c]	*hkl*[a]	d_{obs}[b]	d_{calc}	I_{obs}[c]
100	s	1.554	s	001	s	0.585	
010	s	1.136	s	111	0.492	0.493	M
110	0.917	0.917	VS	201	0.466	0.467	M
200	0.779	0.777	S	211	0.433	0.432	M
210	0.639	0.641	VS	121	0.397	0.394	S
020	0.567	0.568	VW	411	0.311	0.312	W
120	0.533	0.533	S	511	0.269	0.267	W
300	s	0.515	s				
320	0.384	0.383	W	002	0.293	0.293	VW
030	s	0.379	s	112	0.280	0.279	W
410	0.369	0.368	M	202	0.272	0.274	W
230	0.339	0.340	W	312	0.249	0.248	M
510	0.301	0.300	M				

[a] Indexed on an orthorhombic unit cell with parameters $a = 1.554 \pm 0.002$ nm, $b = 1.136 \pm 0.002$ nm, and c (chain axis) $= 0.585 \pm 0.02$ nm. [b] s = systematic absence. [c] VS = very strong, S = strong, M = medium, W = weak, VW = very weak.

lamella or limited stacks of lamellae deposited with random azimuthal orientations relative to the lamellar normal.

The diffraction signal indices, spacings, and estimated relative intensities are given in Table 2. The diffraction signals on the first- and higher-layer lines are broader as a consequence, we believe, of the shorter (≈7 nm) coherence length along the molecular axis. The wide-angle X-ray diffraction pattern obtained with the incident beam directed orthogonal to the melt-crystallized PDTD fibers is shown in Figure 3b. The pattern is similar to that obtained from the sedimented mats of isothermally solution-grown crystals (Figure 3a), except that the diffraction signals (*hk*1) on the first-layer line are sharper, a feature that we will consider in the Discussion section later. The equatorial diffraction signals match those obtained by electron diffraction and confirm that the electron diffraction pattern (Figure 2a) represents the *hk*0 reciprocal lattice. Systematic absences for *h*00 and 0*k*0 for odd *h* and *k*, respectively, were found.

With knowledge of the spacings and indices of the *hk*0 diffraction signals we were able, by following the row lines, to unambiguously identify six independent *hk*1 first-layer-line signals (see Table 2). The measured spacings of these *hk*1 diffraction signals were used to establish, with confidence, a *c*-value of 0.585 ± 0.002 nm. Second-order layer line diffraction signals also appear, including a weak (002) meridional diffraction signal (see Table 2). This distribution of layer line intensity suggests a 2-fold helical conformation for the PDTD molecule, which when coupled with the other systematic absences mentioned above, enables the space group $P2_12_12_1$ to be assigned. The diffraction signals in both patterns (Figure 3a and b) index on an orthorhombic unit cell with parameters $a = 1.554 \pm 0.002$ nm, $b = 1.136 \pm 0.002$ nm, and c (chain axis) $= 0.585 \pm 0.002$ nm. The wide-angle X-ray diffraction pattern obtained with the incident beam orthogonal to the sedimented mat surface shows a set of diffraction rings that index on the same crystallographic lattice. A summary of the measured diffraction spacings, indexing, and relative intensities are given in Table 2.

The low-angle X-ray diffraction pattern (Figure 3c) shows a pair of arcs on the meridian, at a spacing of 7.26 ± 0.03 nm, that we believe represents the lamellar stacking periodicity (LSP). We are able to record this pattern simultaneously with the 110 wide-angle diffrac-

tion signal, allowing for a direct calibration, and, therefore, to measure the LSP spacing with better than usual confidence.

Discussion

Backbone Conformation. The evidence from the oriented X-ray diffraction patterns suggests a 2-fold-helical conformation for the backbone of PDTD molecules. The observed intensity distributions in both the electron and X-ray diffraction patterns indicate that two molecules pass through the *ab* basal plane at the corner(s) and center,[10] implying that the crystal has four chemical units per unit cell. Indeed, the assignment of space group $P2_12_12_1$ defines the coupling between molecules rather precisely and means that the molecules are arranged in an antiparallel fashion. The measured value of $c = 0.585$ nm is 22% lower than expected for an all-trans polymethylene backbone conformation with substituents located on every third carbon atom (see Introduction). This suggests that the backbone conformation is somewhat compressed by the introduction of gauche bonds. Density calculations, based on the measured unit cell dimensions and space group symmetry, wholly support such a structure. However, we are aware that an all-trans backbone conformation (*c*-repeat of 0.75 nm) has been proposed for the somewhat related family member oligo(fluoren-9,9-diyl-*alt*-ethane-1,2-diyl)s (see Introduction) on the basis of NMR data.[5] As a consequence of this proposed structure, we wish to take special care when considering the backbone conformation of poly(diethyl trimethylene-1,1-dicarboxylate). If, for the sake of argument, we imagine an all-trans backbone conformation (*c*-repeat of 0.75 nm) for PDTD, the calculated fully crystalline density would be 0.93 g·cm^{-3}, a value 21% less than the measured value of 1.17 ± 0.03 g·cm^{-3}. Because calculated densities are invariably greater than measured densities, this would be a serious and fundamental problem for a crystalline structure of PDTD based on an all-trans backbone conformation. Thus, we are confident that PDTD backbone conformation is axially compressed (by 22%) and not all-trans.

It should also be mentioned that the chemical shift evidence previously reported for poly(fluoren-9,9-diyl-*alt*-ethane-1,2-diyl) oligomers[5] cannot really distinguish between a $GT\bar{G}GT\bar{G}$ sequence and an all-trans backbone conformation. The reported experimental results indicate that the fluorenyl moieties face each other and are spatially close, which is the case in both conformations. It is also possible that these systems adopt different conformations in solution and in the solid state. Clearly, further experimental investigations will be needed before unambiguous and firm conclusions can be obtained on the rules governing the conformations of macromolecules characterized by this unusual substitution pattern.

For polymers in which the side groups have the potential flexibility to decouple themselves from the symmetry of the backbone, as is the case for PDTD, it is also prudent to consider whether the side groups within the crystal could conspire in some way to generate unexpected periodicities. The side group atoms in poly(diethyl trimethylene-1,1-dicarboxylate) can potentially represent up to 66% of the total scattering (the first carbon atom of each side group X will *not* be independent of the backbone conformation). We have found that, in modeling and packing calculations, only about half of the total side group atom scattering has the potential to decouple from the backbone symmetry. However, despite extensive efforts, we were unable to find any structures that would generate even the basic features of the experimental diffraction pattern while maintaining an all-trans backbone conformation.

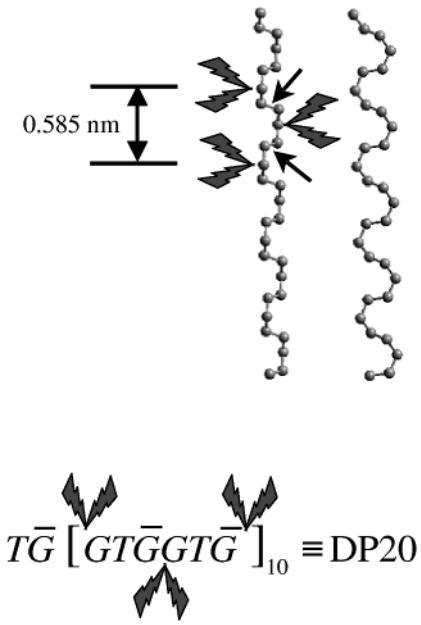

Figure 4. Two orthogonal views (perpendicular to the *c*-axis) of the basic backbone ($GT\bar{G}GT\bar{G}$) conformation for poly(diethyl trimethylene-1,1-dicarboxylate). This backbone conformation is a 2-fold helix with a *c*-repeat of 0.585 nm. Note that the trans conformations (arrowed) are the central dimethylene $CX_2-CH_2-CH_2-CX_2$ bonds in the structure. The shaded side features represent the −X side groups.

The structural model in which the backbone conformation is compressed has a calculated density of 1.20 g·cm^{-3}, giving an appropriate fit with the measured density (3% more than the measured value). In accordance with the concepts outlined in the Introduction, chain conformations were considered involving combinations of trans and gauche bonds while still maintaining the 2-fold helical character for the backbone. It turns out that the backbone sequence $GT\bar{G}GT\bar{G}$ meets these two criteria exactly, and this basic conformation is illustrated in Figure 4 and 5a.[11]

The backbone conformation sequence *GTGGTG* was also considered because it is also capable of generating a *c*-repeat commensurate with the measured value of 0.585 nm. However, as illustrated in Figure 5b, such a backbone conformation does not exhibit the 2-fold screw symmetry required by the $P2_12_12_1$ space group. Thus, only the backbone conformation sequence $GT\bar{G}GT\bar{G}$ meets the requirements of the electron and X-ray diffraction data.

At this stage, the potential energy profiles of the torsional angles for $CX_2-CH_2-CH_2-CX_2$, $-CH_2-CX_2-CH_2-CH_2-$, and $CH_2-CH_2-CX_2-CH_2$ bonds were calculated. We wished to ensure that conformation sequence $GT\bar{G}GT\bar{G}$ is indeed both energetically and stereochemically feasible, i.e., that the backbone is comfortably in an energy minimum rather than being driven into this conformation by side group packing considerations. This could be the case if not all possible chain conformations were examined during the structural modeling process. The calculated potential energy profiles for the torsional angles are plotted in Figure 6.

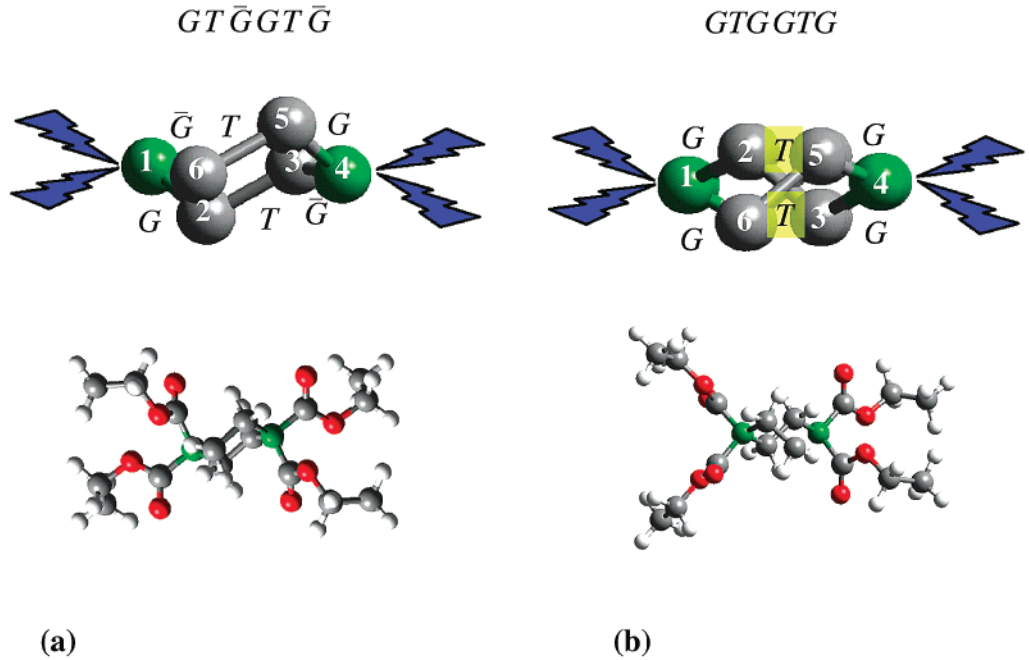

Figure 5. (a) Detailed view (parallel to the chain *c*-axis) highlighting the 2_1-helical character of the proposed $GT\bar{G}GT\bar{G}$ conformation; the order of the torsional angles (top) is given. Note that adjacent side groups on a given carbon atom have different geometries (bottom). (b) Similar views of the *GTGGTG* conformation, also capable of generating the periodicity of 0.585 nm. This conformation is not a 2_1-helix.

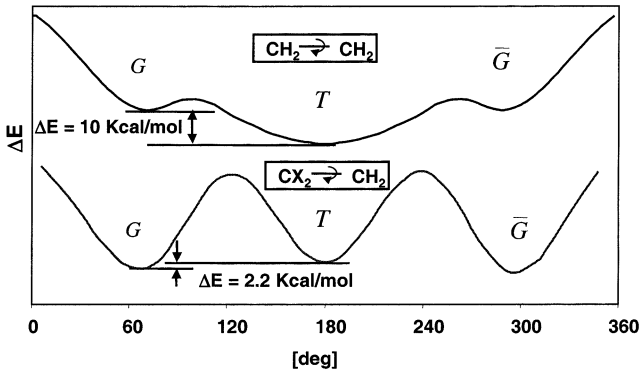

Figure 6. Calculated potential energy profiles for the various bond torsional angles: (a) $-CH_2-CH_2-$ bond, showing the lower minimum for the *T* conformation, and (b) lower energy of the gauche bonds, adjacent to the CX_2 unit.

It can be seen that, for the $CX_2-CH_2-CH_2-CX_2$ bond, the trans conformation is noticeably preferable. However, the situation is different for the $-CH_2-CX_2-CH_2-CH_2-$ and $CH_2-CH_2-CX_2-CH_2$ bonds; in these cases, the *G* and $\bar{G}$ conformations are marginally (2.2 kcal·mol^{-1}) favored. Thus, these results provide supporting evidence for the proposed $GT\bar{G}GT\bar{G}$ backbone conformation sequence favored by the X-ray diffraction data. It should be noted that this backbone conformation imparts a direction to the chain in addition to the different terminal end groups.

Consideration of Side Group Geometry. Figure 7a and b illustrates the situation if the carbon and oxygen atoms in the pair of ethyl carboxylate side groups are arranged in a plane orthogonal to the polymeric backbone. The adjacent ethoxy oxygen atoms clash (interatomic distance of 0.16 nm), and as a consequence, countertorsional rotations of ≈60° about the C−C−C═O bonds are necessary to relieve congestion, as shown in Figure 7c and d.

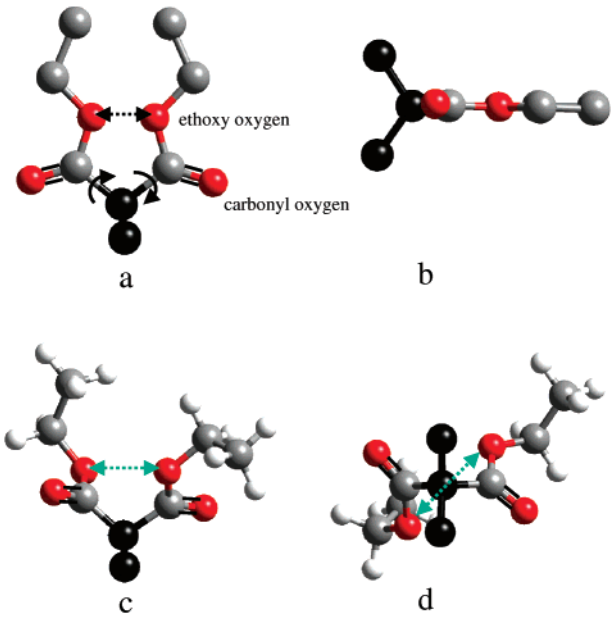

Figure 7. (a, b) Two orthogonal views, parallel and perpendicular to the *c* axis, of the carbon and oxygen atoms for the pair of $-COOC_2H_5$ side groups if all of the atoms lie in a plane orthogonal to chain axis. Backbone chain carbon atoms in black. This conformation is not sterically feasible because the two adjacent ethoxy oxygen atoms are too close (arrowed distance). Thus, torsional rotations occur about the C−C−C═O bonds, as illustrated by curved arrows, to relieve congestion. (c, d) Two orthogonal views, parallel and perpendicular to the *c*-axis, showing the final conformation of the side groups. Backbone chain carbon atoms in black. In this case there is no interatomic clash between the ethoxy oxygen atoms.

Chain Packing and Crystal Structure Refinement. Two energy minimized PDTD chain segments were placed into the orthorhombic unit cell subject to symmetry requirements, and the initial setting angle(s) (in the *ab*-plane) were found by best fit with the observed electron and equatorial X-ray diffraction intensities. The

Table 3. Comparison of Measured (F_{hkl}^{mea}) and Calculated (F_{hkl}^{cal}) *hkl* Structure Factors of Electron Diffraction Signals from a PDTD Lamellar Crystal to 1/0.3 nm^{-1} [a]

hkl	F_{hkl}^{mea}	F_{hkl}^{cal}
110	134.2	146.8
120	104.9	118.1
200	126.5	136.0
210	119.6	114.1
130	56.8	37.7
220	48.3	43.8
230	54.8	45.4
310	38.7	31.6
320	58.3	75.0
400	87.4	75.0
410	68.5	65.3
420	29.8	41.3
510	16.1	10.3
020	26.5	26.7

[a] Calculated *R* value = 0.135.

Table 4. Torsional Rotation Angles for the Backbone and Side Group Bonds in the Refined PDTD Crystal Structure

backbone	angle (deg)	side group[a]	angle (deg)
$CX_2-CH_2-CH_2-CX_2$	160 (*T*)	$CH_2-CX_2-C=O$	0 (for X1), 120 (for X2)
$CH_2-CH_2-CX_2-CH_2$	72 (*G*)	$CX_2-C_c-O-CH_2$	176 (*T*)
$CH_2-CX_2-CH_2-CH_2$	−71 ($\bar{G}$)	$C_c-O-CH_2-CH_3$	−100 (for X1), 80 (for X2)

[a] C_c = carbonyl side group carbon atom.

full set of observed X-ray *hkl* intensities were then used to search for possible relative *z*-shifts of the molecules. For each of the contending starting structures, the potential energy of the whole crystal structure was minimized until we were satisfied that we had established the best fit with the experimental data for a model with no stereochemical clashes and minimum potential energy (Table 3). The final torsion angles for the backbone and side chains are given in Table 4. It should be noted that the refined values for the backbone torsional angles in PDTD are about 10° off the formal gauche values and 20° off the trans value for $CX_2-CH_2-CH_2-CX_2$ dimethylene bond. This backbone conformation gives a closer fit with the experimental intensities and matches the measured *c*-repeat exactly. Interestingly, Alder[12] has also noticed a similar off-trans perturbation for the dimethylene bond in oligo(fluoren-9,9-diyl-*alt*-ethane-1,2-diyl)s. The calculated *hk*0 electron diffraction pattern for final structure is shown in Figure 2b for convenient comparison with the experimental pattern. A *R* value of 0.135 is obtained from a comparison of the measured and calculated *hk*0 electron diffraction structure factors out to 0.3 nm (see Table 3). The computer-simulated wide-angle X-ray diffraction pattern is compared with the experimental pattern in Figure 8. As can be seen, the match is good.[9] Two projections of the crystal structure are shown in Figure 9. Thus, in the case of poly(diethyl trimethylene-1,1-dicarboxylate), we judge that it is the mutual interactions between the pair(s) of $-COOCH_2CH_3$ side groups that, in turn, control the backbone conformation.

Nature of the Lamellar-like Crystals. The electron microscopic images of the PDTD crystals grown by isothermal crystallization from benzene (Figure 1) show a constant thickness over the whole crystal surface (on the order of square microns). This constant thickness feature is also supported by the occurrence of the discrete low-angle (LSP) diffraction signal obtained from sedimented mats; indeed, it provides us with a direct measure of the *maximum* crystal thickness of 7.26 ± 0.03 nm. We know, from both electron and X-ray diffraction, that the PDTD molecules are directed orthogonal to the large crystal surface (*ab*-plane) and that the molecules pack in an antiparallel fashion. Figure 10a and b shows views of the PDTD lamellar-like crystals. The outer limit thickness of the crystal is 7.23 nm for PDTD molecules with 20 monomers.[13] We suggest that the degree of molecular dispersion in these PDTD crystals, which were isothermally crystallized from benzene, is small. The experimental support for this statement is the relative sharpness of the LSP arc width (Figure 3c) and the relative smoothness of the crystal surfaces[14] (see Figure 1). For example, if a number of PDTD molecules with DP = 21 were incorporated into the crystalline lamellae, the measured LSP value of 7.26 ± 0.03 nm would be compromised, because such molecules would tend to increase the mean LSP value by 0.293 nm, an order of magnitude greater than the upper error limit. Thus, PDTD molecules with DP > 20 would cause interlamellar congestion, a feature not consistent with the experimental evidence. Figure 10c conveniently illustrates that the terminal −S−Ph group can fit into the PDTD crystalline lattice without frustrating the crystal,[15] and so, a proportion of the molecules in the crystal could have DP < 20 without an overall noticeable effect in the images and diffraction data. On general grounds, it is perhaps, not too surprising to discover that these crystals, isothermally grown from solution, are close to monodisperse entities. The very nature of this crystallization process is selective. Other rather ill-defined aggregates occur that presumably incorporate molecules with slightly different lengths.

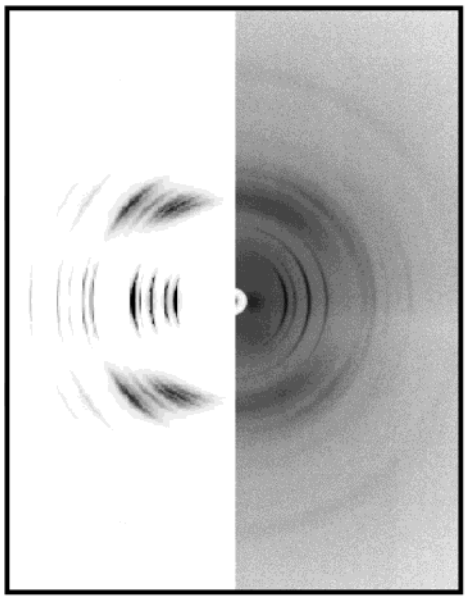

Figure 8. Computer simulated X-ray diffraction pattern from refined model (left) compared with the experimental X-ray pattern (right).

In the case of the melt-crystallized PDTD sample, a wider molecular length range is expected to crystallize out; indeed, the X-ray diffraction results support this expectation. The wide-angle X-ray diffraction pattern (Figure 3b) of melt-crystallized PDTD, although it represents the same crystal structure as the solution-grown crystals, has noticeably sharper *hkl* diffraction

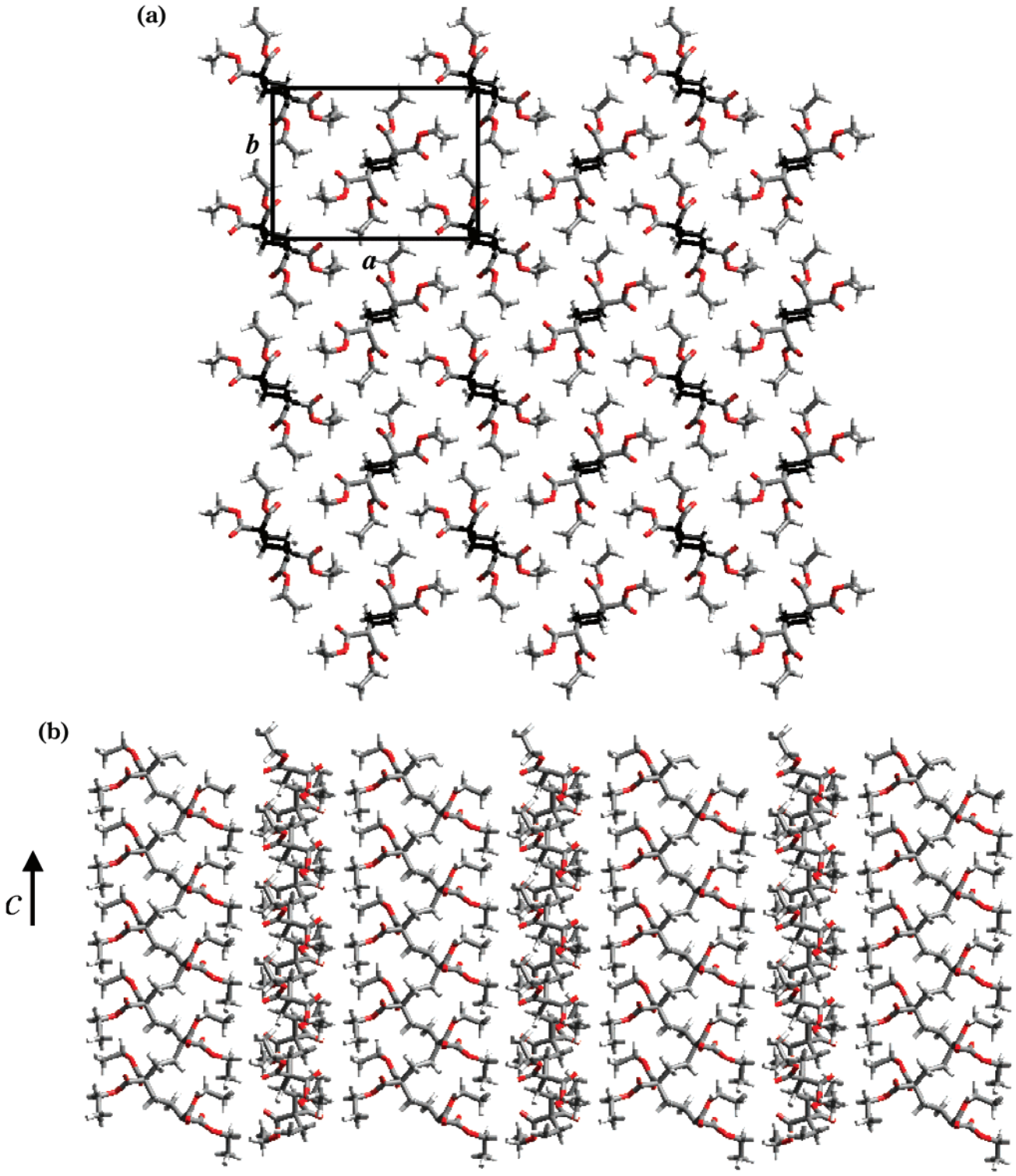

Figure 9. Views of the refined structure of the PDTD crystal in stick mode. (a) Parallel to the *c* axis; the backbone is highlighted in black. The unit cell contains two antiparallel molecules or four PDTD monomers. (b) View orthogonal to the diagonal (110) plane (*c*-axis vertical) showing, successively, corner and center (antiparallel) chains.

signals for $l \neq 0$. Also, we do not observe a LSP signal in the low-angle diffraction region. These results are consistent with crystals in which no segregation takes place into semetic-like layers that are orthogonal to the molecular axis. Rather, we envision an architecture in which the PDTD molecules (see Figure 10c), but in this case with a larger range of individual lengths, can interpenetrate. Although such a structure has incorporated defects[16] (terminal groups), the overall coherence length in the *c* direction is increased, and consequently, the *hkl* diffraction signals for $l \neq 0$ sharpen.

General Considerations Relating to Decorated Alkanes. If alkane-based polymers in the all-trans extended backbone conformation are decorated with a side group(s) on every second backbone carbon atom, interatomic clashes can occur between the contiguous side groups (only ≈0.25 nm apart) along the chain. This congestion is often relieved by the introduction of

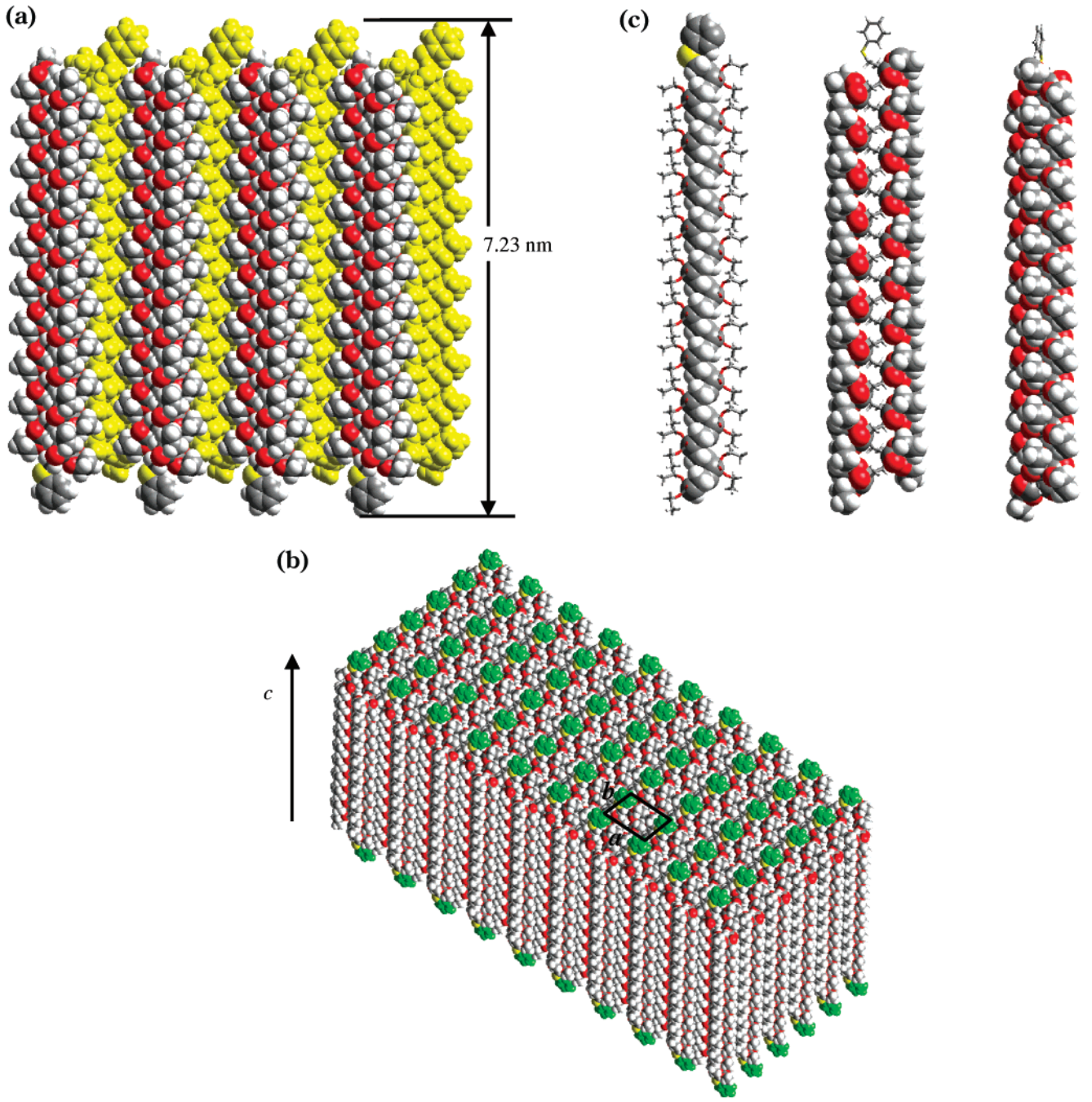

Figure 10. Space-filling model of the lamellar-like crystal structure. (a) View orthogonal to the chain axis (vertical) for a complete 20 DP molecule of PDTD (upward pointing chains in yellow). Note the terminal phenyl rings connected via a sulfur atom to the molecular chain. The outer limit thickness is 7.23 nm (lamellar stacking periodicity (LSP) = 7.26 nm). (b) Oblique view showing the crystal surface; sulfur atom yellow, phenyl ring green. (c) Single PDTD chain (*c* axis vertical) of DP 20: (left) backbone atoms in space-filling mode and side groups in stick mode; (center) backbone atoms in stick mode and side groups in space-filling mode; (right) center chain rotated $\pi/2$ around the *c*-axis.

backbone gauche bonds, e.g., as for *i*-polypropylene[17] and *i*-polystyrene,[18] where the backbone conformation is $(TG)_3$. When the backbone repetitive decoration frequency is reduced, the distances between spatially near-neighbor side groups jumps dramatically to ≈0.75 nm[19] for decoration on every third backbone carbon atom (the polycyclopropanes) and to ≈0.50 nm[19] in the case of decoration sites on every fourth backbone carbon atom. For these families of polymers, the interatomic interactions between side group and backbone atoms will be the primary mechanism for influencing and controlling the overall conformation.[6]

Conclusions

Molecules of poly(diethyl trimethylene-1,1-dicarboxylate), with the formula $Ph{-}S{-}[CH_2{-}CH_2{-}C(COOC_2H_5)_2]_n{-}H$, have been crystallized from benzene by isothermal crystallization at 30 °C. The molecules have an average DP of ≈20 and a polydispersity of 1.13. The lamellar-like crystals are ellipsoidal in shape (≈4 $\mu \times 1\ \mu$m in lateral dimensions) but only 7.3 nm in thickness. Judging from X-ray diffraction and electron microscopic evidence, the crystals are composed of molecules aligned orthogonal to the lamellar surface and pack in an antiparallel arrangement in a two-chain

orthorhombic unit cell. The constant thickness of the crystals, as deduced from low-angle X-ray diffraction of stacked lamellae and from in electron microscopy imaging, suggests that, under the crystallization conditions used, DPs at, or close to, 20 were selectively crystallized.

No such molecular length selectivity was evident in melt-crystallized samples; in this case, the whole molecular length dispersion range crystallized to form crystals with a longer average coherence length in the molecular *c*-axis direction. The lateral space demanded by the side group decoration means that the terminal phenyl group can easily be accommodated in the crystalline lattice.

We have discovered that the molecular backbone conformation has a torsional angle sequence close to $GT\bar{G}G\bar{T}G$, with the trans bonds at the dimethylene $C-CH_2-CH_2-C$ sites. This conformation generates a 2-fold helix with a pitch that matches the measured crystallographic *c*-repeat of 0.585 nm. In the case of poly(diethyl trimethylene-1,1-dicarboxylate), it would appear that the mutual interactions of the pair(s) of $-COOCH_2CH_3$ side groups influence the backbone conformation.

To our knowledge, this is the first occasion in which a backbone conformation for a substituted polytrimethylene has been unambiguously determined.

Acknowledgment. We thank the Engineering and Physical Sciences Research Council (U.K.) for supporting this research, including a postdoctoral research fellowship to P.S.; the NSF-funded UMass Materials Research Science and Engineering Center (MRSEC, DMR 98-09365) for support; and the 3M company for a 3M Yound Faculty award to J.P. Part of this collaborative venture was undertaken when E.A. was Visiting Professor at the Department of Polymer Science and Engineering, University of Massachusetts at Amherst. We are very grateful to Dr. Xie Tao for his help in the synthesis and characterization of the polymeric sample.

References and Notes

(1) Bunn, C. W. *Proc. R. Soc. (London)* **1942**, *A180*, 67.
(2) Natta, G.; Corradini, P.; Bassi, I. W. *J. Polym. Sci.* **1961**, *51*, 505. Tadokoro, H. *J. Polym. Sci.* **1966**, *C15*, 1. Also see, for example: Alexander, L. E. *X-ray Diffraction Methods in Polymer Science*; Wiley-Interscience: New York, 1969. Tadokoro, H. *Structure of Crystalline Polymers*; Wiley: New York, 1979.
(3) Bunn, C. W.; Howells, *J. Polym. Sci.* **1955**, *18*, 307.
(4) Natta, G.; Corradini, P.; Bassi, I. W. *Nuovo Cimento, Suppl. 1* **1960**, *15*, 68.
(5) Alder, R. W.; Anderson, K. R.; Benjes, P. A.; Koutentis, P. A.; Orpen, A G. *J. Chem. Soc., Chem. Commun.* **1998**, 309.
(6) Alder, R. W.; Allen, P. R.; Anderson, K. R.; Butts, C. P.; Khosravi, E.; Martin, A.; Maunder, C. M.; Orpen, A G.; St. Pourcain, C. B. *J. Chem. Soc., Perkin Trans. 2* **1998**, 2083.
(7) Penelle, J.; Herion, H.; Xie, T.; Gorissen, P. *Macromol. Chem. Phys.* **1998**, *199*, 1329.
(8) Penelle, J.; Xie, T. *Macromolecules* **2000**, *33*, 4667.
(9) Historically, structures of polymers have been tested for goodness of fit using a single number reliability index, *R*, by summing the differences, $\sum|\Delta F|$, between measured and calculated structure factors and normalizing. It should be borne in mind that a random acentric structure based on a model with the correct number and type of atoms yields a theoretical *R* value of 0.59 (see, for example: Wilson, A. J. C. *Acta Crystallogr.* **1950**, *3*, 397), so a perfect fit is when $R = 0$, and from a stereochemical point of view, $R = 0.59$ represents a meaningless structure. Thus, the values of *R* in the range 0.3−0.2, which are values published for many polymeric crystal structures, do not instill particular confidence with respect to the goodness of fit or proof of structure. [*Embarrassingly, one can find published polymer structures in which not all of the appropriate diffraction signals (out to the claimed resolution limit in reciprocal space) are included in the $\sum|\Delta F|$ term, below intensity threshold values in the experimental data set, for example. Such a procedure gives a false lowering of the *R* value.] In practice, we find the overall fit using the Cerius simulation method to be a truer judge of fit between experiment and calculation. It is akin to a two-dimensional facial recognition process, and as humans, we are experienced in noticing discrepancies between two side-by-side images, as, for example, in comparing the two halves of Figure 8. We have, however, also provided an *R* value for *hk*0 electron diffraction signals in Table 3.
(10) In the formal description of the $P2_12_12_1$ space group (see *International Tables for Crystallography*; Kynock Press: Birmingham, England, 1968; Vol. 1) the origin is displaced to halfway between the three pairs of nonintersecting 2-fold screw axes. For convenience and a more appropriate description of our PDTD structure, we have moved the chains to the corner and center positions in the unit cell *ab*-face.
(11) At this stage, the calculated *c*-repeat is within 0.9% of the measured X-ray diffraction value. Also, we show later that the *T* conformation is necessary for the $CX_2-CH_2-CH_2-CX_2$ bond.
(12) Professor R. W. Alder, Chemistry Department, University of Bristol, Bristol, U.K. Private communication.
(13) The single diffraction order of the LSP suggests that the lamellar-like crystals are stacking with random azimuthal orientations about their surface normal.
(14) The electron microscopic images shown in Figure 1 are coated with metal to enhance the contrast; however, untreated crystals exhibit a similar surface smoothness.
(15) We shall show that this happens in the case of the melt-crystallized samples later.
(16) Because, in the case of PDTD crystals, even the bulky terminal group −S−Ph (see Figure 9) can sit comfortably in the crystal lattice (see Figure 10), no significant lattice distortion occurs (similar to vacancies in metals).
(17) Turner-Jones, A.; Cobbold, A. J. *J. Polym. Sci. B* **1968**, *6*, 539. Samuels, R. J.; Yee, R. Y. *J. Polym. Sci. A2* **1972**, *10*, 358.
(18) Natta, G.; Corradini, P. *Makromol. Chem.* **1955**, *16*, 77. Natta, G.; Corradini, P.; Bassi, I. W. *Nuovo Cimento, Suppl. 1* **1960**, *15*, 68.
(19) Nearest-neighbor side group distance on one side of the planar carbon atom backbone all-trans conformation.

MA020486Z